Image Cover Sheet

CLASSIFICATION	SYSTEM NUMBER
UNCLASSIFIED	146069

TITLE

A SIMPLE MODEL FOR THE PREDICTION OF PHASE SWINGS OBSERVED IN ACOUSTIC PROPAGATION DATA

AN:94-06122

System Number:

Patron Number:

Requester:

Notes:

DSIS Use only:

Deliver to: BA

Defence Research Establishment Pacific
Centre de recherches pour la défense pacifique

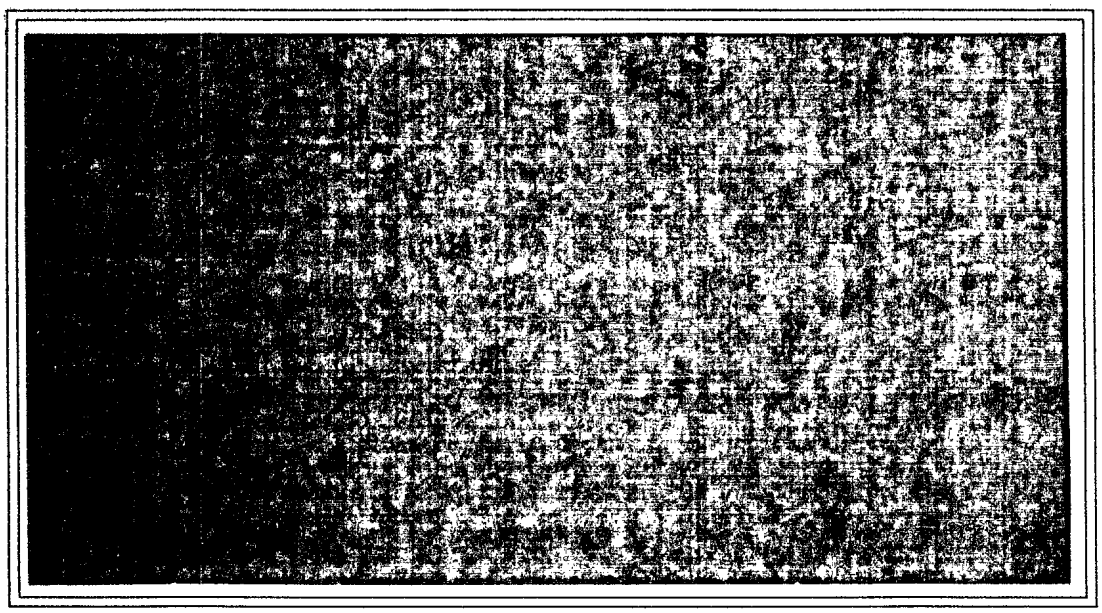

DEFENCE RESEARCH ESTABLISHMENT PACIFIC

Research and Development Branch
Department of National Defence

Canada

Defence Research Establishment Pacific
Centre de recherches pour la défense pacifique

DEFENCE RESEARCH ESTABLISHMENT PACIFIC

CFB Esquimalt, FMO Victoria, B.C. V0S 1B0

Technical Memorandum 94-117

A SIMPLE MODEL FOR THE PREDICTION OF PHASE SWINGS OBSERVED IN ACOUSTIC PROPAGATION DATA

by

B.H. Maranda and G.R. Ebbeson

July 1994

Approved By:

Chief DREP

Research and Development Branch
Department of National Defence

Canada

ABSTRACT

In 1986, a propagation loss experiment was conducted in which a narrowband source moved away from two widely separated hydrophones located in shallow water. It was found that the relative phase between the signals received at the two hydrophones underwent rapid swings near the nulls of the pressure field. In this paper, a simple two-mode propagation model is derived that explains the source of these phase swings. In order to produce phase swings as large as those observed in the experimental data, it was necessary to introduce different bathymetries along the propagation paths to the two hydrophones.

RÉSUMÉ

En 1986, on a effectué une expérience acoustique dans laquelle une source à bande étroite s'éloignait de deux capteurs situés en eau peu profonde, la séparation entre les capteurs étant grande. On a constaté que la phase relative entre les signaux reçus aux capteurs subissait une fluctuation rapide aux points où le champ de pression atteignait ses minima. Dans cet article, nous développons un modèle basé sur deux modes normaux qui explique la source de ces fluctuations de phase. Pour produire des fluctuations qui sont aussi grandes que celles observées dans les données expérimentales, il était nécessaire d'introduire profondeurs différentes le long des trajets de propagation aux deux capteurs.

1. INTRODUCTION

In 1986, an acoustic experiment was carried out in which a narrowband source moved away from an array of hydrophones located in shallow water. As part of the analysis of the data collected during the experiment, the pressure magnitudes and relative phases along the array were computed. It was found that when the hydrophone separation was large, the relative phase periodically underwent a substantial perturbation, or swing. Furthermore, it was observed that these swings occurred when the pressure amplitudes went through a minimum. In this paper, a simple model is derived that elucidates the source of the phase swing.

In the next section, the acoustic experiment is described in detail and the experimental data are presented. In Sec. 3, the model is derived and the experimental results are compared with those produced by this theoretical model. Finally, a summary is provided in Sec. 4.

2. THE EXPERIMENTAL DATA

The acoustic data presented in this paper were obtained from a propagation loss experiment that was carried out in a continental shelf environment. During the experiment, a receiving system was located in about 500 m of water on the shelf. Figure 1 shows a schematic of the postions for two of the hydrophones in that system. For this analysis, they will be referred to as hydrophones x and y. These hydrophones were fixed at a depth of 100 m and separated horizontally by a distance of 1500 m. The source was towed outward from the receivers into the deeper waters of the continental slope along a bearing that was parallel to the broadside direction for the two hydrophones. It generated a continuous-wave signal at a frequency of 24 Hz. Because of the horizontal offset between the tow and broadside directions, the angle of incidence β for the sound arriving at the hydrophones ranged between 4° and 3° for source ranges between 110 and 163 km respectively. That is, the source appeared to move closer to broadside as the range increased. In the figure, $1500 \sin\beta$ is a measure of the distance between hydrophone y and the plane wavefront (dashed line) along the direction of the propagation.

Figure 2(a) shows a plot of the received level vs source range for the two hydrophones. To aid in clarity, the results for hydrophone y are indicated with a dashed line. Because of the small variations in the Doppler-shifted frequencies due to changes in the source speed, the signal at each hydrophone was "tracked" in frequency throughout the range interval by determining its peak level over a number of adjacent frequency bins. It should be noted that the signal-to-noise ratios for these data were sufficiently large that this tracking routine never lost the signal in the ambient noise. The results for both hydrophones show

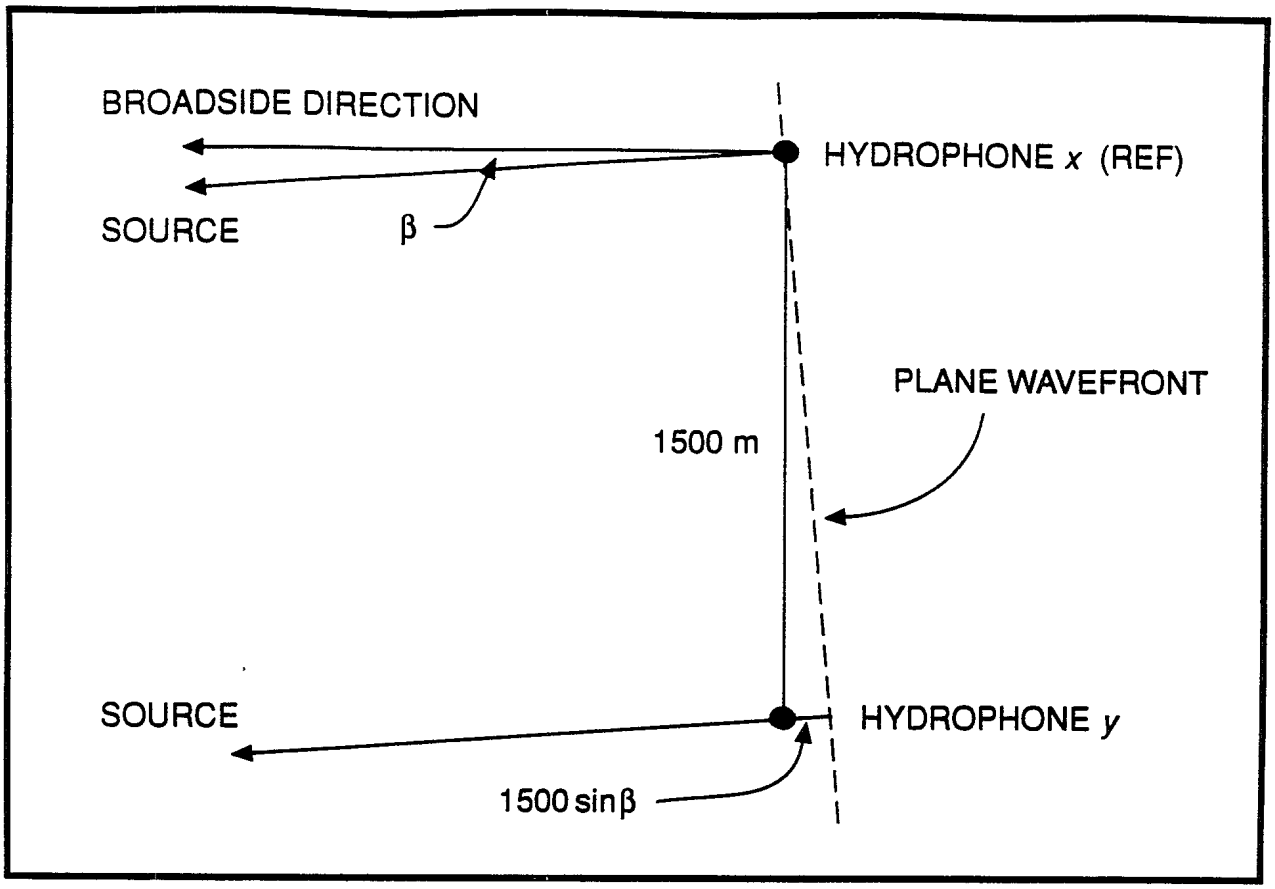

Fig. 1. Schematic showing the hydrophone positions and the direction to the acoustic source.

the familiar interference pattern with range that is generally associated with the interaction between two dominant modes in a shallow water waveguide.[1] Simulations with the normal-mode propagation model SNAP[2] using the measured environment for the experimental site revealed that this modal interference was due to the two lowest-order modes (modes 1 and 2). It is believed that the higher-order modes were rapidly attenuated by the increased interaction with the bottom during the propagation up the continental slope. From the figure, it is seen that the period of the interference patterns is about 9.5 km and that there is a shift in range of about 1.8 km between the patterns for the two hydrophones.

The relative phase between the signal received on hydrophone y and that on hydrophone x is plotted in Fig. 2(b), also as a function of source range. In these results, the relative phase has been "unwrapped". That is, multiples of 360° have been subtracted from the measured (wrapped) phase difference so that the result represents the total dis-

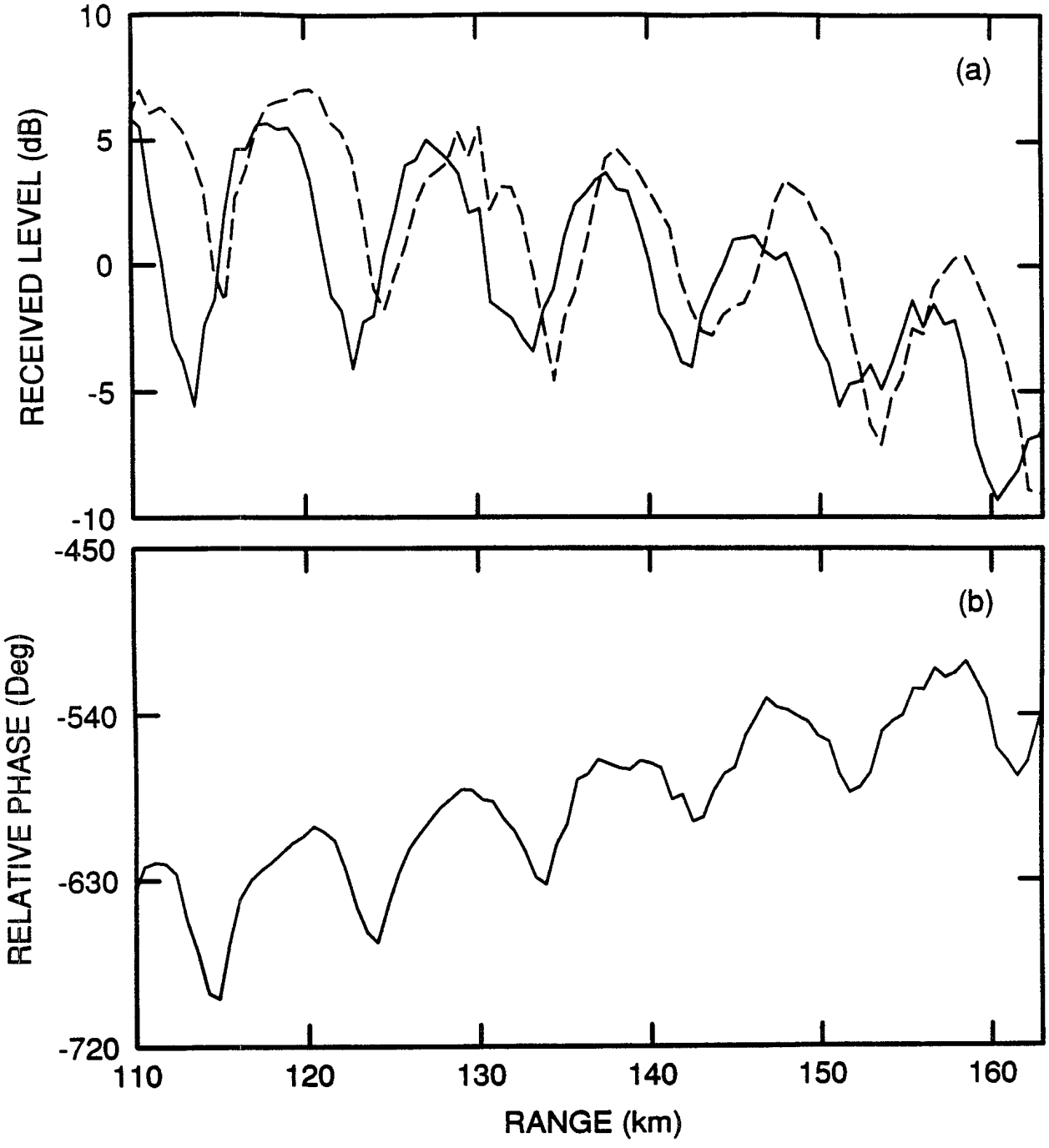

Fig. 2. (a) Received level vs source range for hydrophones x and y (solid and dashed curves respectively). (b) The phase at hydrophone y relative to that at hydrophone x.

tance (360° of phase equals one wavelength of distance) between hydrophone y and the signal wavefront in the direction of the source. From Fig. 1, this unwrapped relative phase would be

$$\theta = -\left(\frac{1500 \sin\beta}{\lambda}\right) 360°. \tag{1}$$

In this equation, the wavelength λ is equal to c_r/f where c_r is the reference sound speed in the water and f is the signal frequency. For example, in the environment of this continental shelf site where $c_r = 1440$ m/s, the 24-Hz signal had a wavelength of $\lambda = 1440/24 = 60$ m. In addition, at a source range of 110 km, the angle of incidence was $\beta = 4°$. Therefore, from Eq. (1), the relative phase at hydrophone y would have been be close to $\theta = -627.8°$. Hence, it was necessary to subtract 720° from the measured phase difference to get the correct unwrapped relative phase shown in Fig. 2(b).

Two observations can be made from the phase results of this figure. First, the magnitude of the relative phase generally decreases with increasing range. This is because the source appeared to move closer to broadside with range (β decreased), which in turn caused the relative phase at hydrophone y to approach zero. Second, there are six negative "phase swings" in the relative phase, and these occur roughly at the six interference nulls of the received signals shown in Fig. 2(a). The magnitude for the swing at a range of 115 km is about 80°. This latter effect, which was not expected, could seriously degrade the performance of a horizontal line array in this shallow-water environment. For example, working from Eq. (1), a swing of −80° in the relative phase can cause an error in the apparent direction of the source of +0.5°. Although small, this bearing error amounts to a lateral range error of 0.96 km at a source range of 110 km. Therefore, it is important to understand fully the cause of this phase swing phenomenon and be able to predict with some degree of accuracy the magnitude of the swings.

3. DEVELOPMENT OF A MODEL

A simple model that explains the basic features of the data will now be developed. The main objective is to derive a model that accounts for the phase variation with sufficient accuracy to explain the phase swings; at the same time, however, we desire a sufficiently simple model that it is possible to obtain analytical insight into the phenomenon.

Given a time-harmonic source of angular frequency ω and depth z_s in the ocean, the resulting pressure observed at a range and depth (r, z) can be expressed as $p(r, z)\, e^{-i\omega t}$. Here $p(r, z)$ is the solution to the time-harmonic (Helmholtz) wave equation, and is referred to as the time-harmonic pressure field, or simply the pressure. A standard representation

for $p(r,z)$ in a range-independent ocean is given by the modal sum

$$p(r,z) = A\sum_{n=1}^{N}\frac{\phi_n(z)\phi_n(z_s)}{\sqrt{k_n r}}e^{ik_n r}, \tag{2}$$

where A is a normalization constant. As seen in Eq. (2), the pressure field is decomposed into a sum of N modes, which are characterized by the wavenumbers k_n and mode functions $\phi_n(z)$. The number and values of these modal quantities depend on such parameters of the waveguide as the sound speed and the density of the media. The modes are traditionally numbered so that the wavenumbers k_n are decreasing; i.e., $k_1 > k_2 > \cdots > k_N$.

3.1 The case of two modes

As indicated in the previous section, the simple beating pattern present in the data of Fig. 2(a) suggests that modes 1 and 2 were dominant. Therefore, we shall examine the case of two modes, writing the pressure as

$$p(r) = \frac{1}{\sqrt{r}}(a_1 e^{ik_1 r} + a_2 e^{ik_2 r}). \tag{3}$$

The dependence on z is not shown explicitly in Eq. (3) because the depth is fixed. The coefficients a_1 and a_2 are allowed to be complex-valued, and we write $a_j = |a_j|e^{\psi_j}$ for $j = 1, 2$. The first step in the analysis is to re-write Eq. (3) in a form that separates the main linear trend of the phase from the local phase fluctations. To this end, define

$$\overline{k} = \tfrac{1}{2}(k_1 + k_2) \qquad \text{and} \qquad \Delta k = \tfrac{1}{2}(k_1 - k_2), \tag{4a}$$

and similarly set

$$\overline{\psi} = \tfrac{1}{2}(\psi_1 + \psi_2) \qquad \text{and} \qquad \Delta\psi = \tfrac{1}{2}(\psi_1 - \psi_2). \tag{4b}$$

In terms of these new quantities, Eq. (3) becomes

$$p(r) = \frac{e^{i(\overline{k}r+\overline{\psi})}}{\sqrt{r}}\left[|a_1|e^{i(r\Delta k+\Delta\psi)} + |a_2|e^{-i(r\Delta k+\Delta\psi)}\right]. \tag{5}$$

The next step is to examine the magnitude and phase of the pressure. We write $p(r) = |p(r)|e^{i\theta(r)}$; then from Eq. (5) it can be shown that

$$|p(r)| = \frac{|a_1| + |a_2|}{\sqrt{r}}\left[\alpha^2 + (1-\alpha^2)\cos^2(r\Delta k + \Delta\psi)\right]^{1/2} \tag{6}$$

and

$$\theta(r) = \overline{k}\,r + \overline{\psi} + \tan^{-1}\left(\alpha\,\tan(r\Delta k + \Delta\psi)\right), \tag{7}$$

where

$$\alpha = \frac{|a_1| - |a_2|}{|a_1| + |a_2|}. \tag{8}$$

It can be shown that $|\alpha| \leq 1$. When $\alpha = \pm 1$ only one mode is present and the pressure magnitude exhibits cylindrical spreading (decay proportional to $r^{-1/2}$). In the general case of two modes, Eq. (6) shows that the peaks in the propagation loss occur at ranges corresponding to $r\Delta k + \Delta\psi = m\pi$ for an integer m, and the nulls at ranges for which $r\Delta k + \Delta\psi = (m + \frac{1}{2})\pi$.

Equation (7) shows the phase separated into a linear term $\overline{k}\, r$, a fixed offset $\overline{\psi}$, and a perturbation term. Now, the phase swings must occur in those regions where the phase undergoes rapid change with range. This comment leads us to examine the derivative of the phase with range, which is given by

$$\frac{d\theta}{dr} = \overline{k} + \frac{\alpha\Delta k}{\cos^2(r\Delta k + \Delta\psi) + \alpha^2 \sin^2(r\Delta k + \Delta\psi)}. \tag{9}$$

The dominant behaviour of the derivative can be found by examining it at the peaks and nulls of the pressure field. The results are

$$\left.\frac{d\theta}{dr}\right|_{peak} = \overline{k} + \alpha\Delta k \qquad \text{and} \qquad \left.\frac{d\theta}{dr}\right|_{null} = \overline{k} + \frac{\Delta k}{\alpha}. \tag{10}$$

Now, when the magnitudes of the two modes are approximately the same, $|a_1| \sim |a_2|$, the magnitude of α is small. In this case it follows from Eq. (10) that the perturbation from a linear phase change is small near the peaks of the pressure field, but can be very large in the vicinity of a null. Moreover, the smaller the value of α, the greater the effect.

Another way of arriving at the same conclusion is to consider the perturbation term in Eq. (7) directly. For the purpose of explanation we set $\Delta\psi = 0$. When α is small, the argument $\alpha \tan(r\Delta k)$ of the arctangent function in Eq. (7) will in general change slowly with r. However, $\alpha \tan(r\Delta k)$ becomes unbounded at the points $r\Delta k = (m + \frac{1}{2})\pi$, and as r increases through one of these points the phase $\theta(r)$ will either increase or decrease rapidly by π (depending on whether α is positive or negative). The points of this form correspond to the nulls in the pressure field, as noted above. Figure 3 is a plot of $\tan^{-1}\left(\alpha \tan(r\Delta k)\right)$ as a function of range r for different values of α. Here Δk was set to give a 10 km cycle distance to the pressure field; i.e., $r\Delta k$ increases by π for a 10-km increase in range. As expected, the phase undergoes a rapid increase near points of the form $r\Delta k = (m + \frac{1}{2})\pi$, the effect becoming more dramatic as α becomes smaller. It is important to note that only the perturbation term in Eq. (7) has been plotted in Fig. 3; the linear part of the phase, $\overline{k}\, r$, may vary by tens of cycles over the distance shown in the figure.

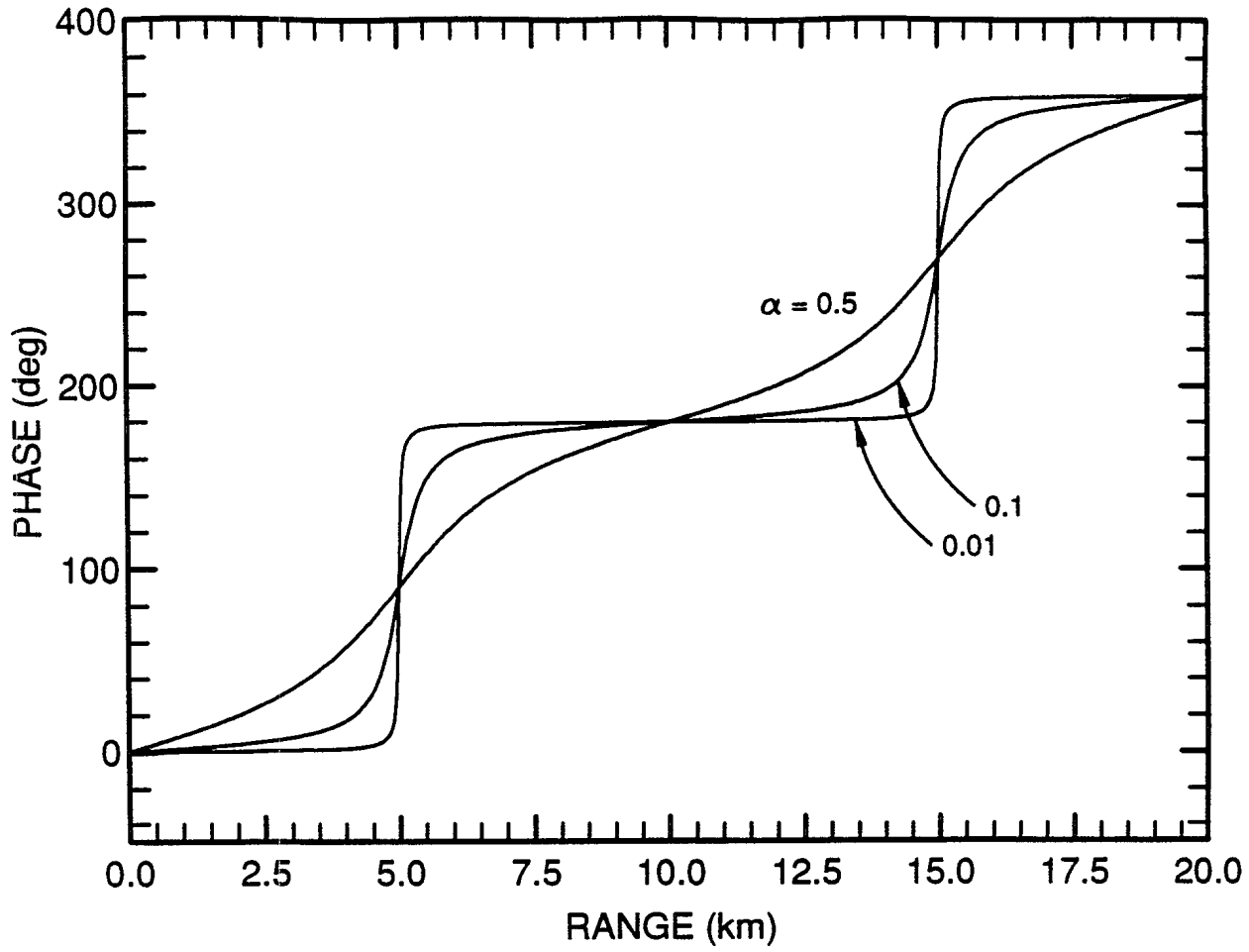

Fig. 3. Perturbation of the phase from a linear trend in a two-mode model. Curves are shown for three values of α.

3.2 Relative phase between two hydrophones

So far we have examined the behaviour of the phase at a single point in the waveguide as the range to the source varies. In practice it is the relative phase between two hydrophones that is important, and we now turn to an examination of this topic. At this point the discussion remains general, and will be related to the experimental data later.

Let the range from the source to hydrophone x be denoted by r and the range to hydrophone y by $r + \Delta r$. If $\Delta r > 0$ hydrophone y is farther from the source than hydrophone x, and if $\Delta r < 0$ it is closer. Our model assumes azimuthal symmetry, so that it is not required that the two hydrophones lie on a radial line from the source. The phase

at hydrophone y relative to that at x is given by

$$\theta_y(r + \Delta r) - \theta_x(r), \tag{11}$$

where θ_x and θ_y are the phases at hydrophones x and y respectively. For the two-mode model with azimuthal symmetry, Eq. (11) is simply the phase difference $\theta(r + \Delta r) - \theta(r)$, where $\theta(\cdot)$ is given in Eq. (7). This difference has a constant offset $\overline{k}\Delta r$ and a fluctuating component due to the last term in Eq. (7). The result of the previous section then makes clear the origin of the observed phase swings, as illustrated in Fig. 4. As above, Δk was adjusted to give a 10 km cycle distance and $\Delta\psi$ was set to zero. Furthermore, we set $|a_2| = \frac{1}{2}|a_1|$, which by Eq. (8) yields $\alpha = \frac{1}{3}$, and chose $\Delta r = -2$ km. The abscissa in Fig. 4 is the range r to hydrophone x, and the upper solid line shows the term $\tan^{-1}\left(\alpha \tan(r\Delta k)\right)$ at that hydrophone. The dashed line shows the term $\tan^{-1}\left[\alpha \tan\left((r + \Delta r)\Delta k\right)\right]$ at hydrophone y. Subtracting the upper solid line from the dashed line yields the relative phase (ignoring the constant phase offset $\overline{k}\Delta r$). It is seen that the phase swings occur because the phase at hydrophone x "jumps" by 180° a distance Δr before the phase at y makes a similar jump. For a fixed range offset Δr, the size of the phase swing is determined by the value of α. For smaller values of α, the magnitude of the phase swing is larger. This is illustrated in Fig. 5, where α was set to 0.1.

3.3 The complete model

Although the origin of the phase swings has now been clarified, the size of range shift between nulls in the real data of Fig. 2(a) cannot be attributed solely to a range offset Δr between hydrophones. Whereas the range offset between the hydrophones was on the order of $-1500 \sin 4° \cong -105$ m for the experimental geometry, the real data show a range shift of approximately -1.8 km between nulls. This is shown more clearly in Fig. 6, which reproduces part of the data from Fig. 2 on a larger scale. Thus the shift in the curves must be explained through some other mechanism.

One possible mechanism that has been identified as the cause for the range shift is differing bathymetries near the receivers. Therefore we relax the constraint of azimuthal symmetry in the model and introduce a difference in bottom depth near the two receivers, as shown in Fig. 7. It should be noted that in reality the source was in deep water over the continental slope. However, in order to keep the model simple, we shall retain the range-independence of the bathymetry near the source. How this affects the modelled results will be discussed later. As seen in the figure, the bottom over which the signal travels to hydrophone x is taken to be flat, with depth d. The pressure at x is then given by the

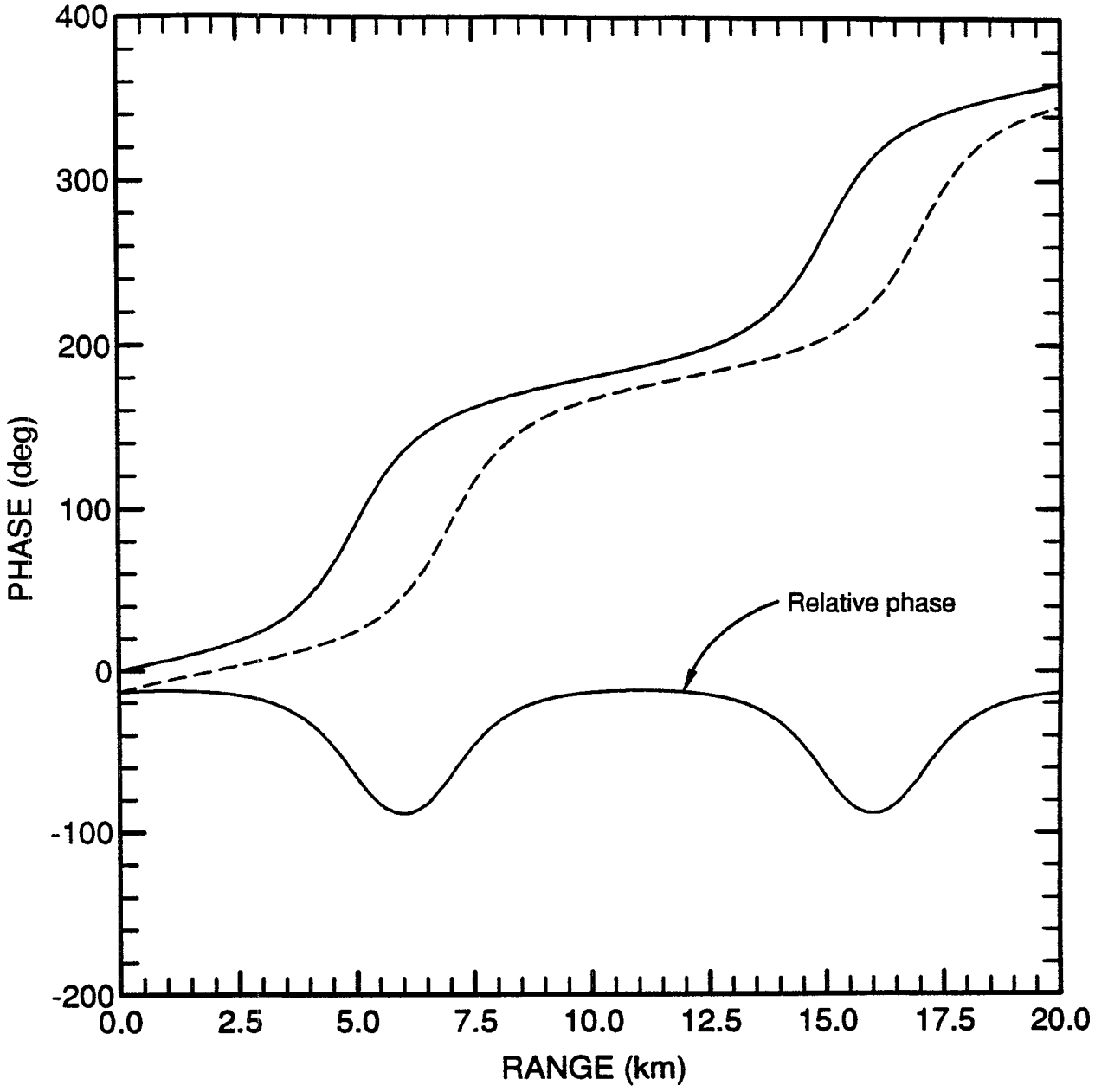

Fig. 4. Illustration of the phase swing in the relative phase. Upper solid and dashed lines are the absolute phases at hydrophones x and y respectively, with $\alpha = \frac{1}{3}$. Lower solid line is the relative phase obtained by subtracting the upper solid line from the dashed line.

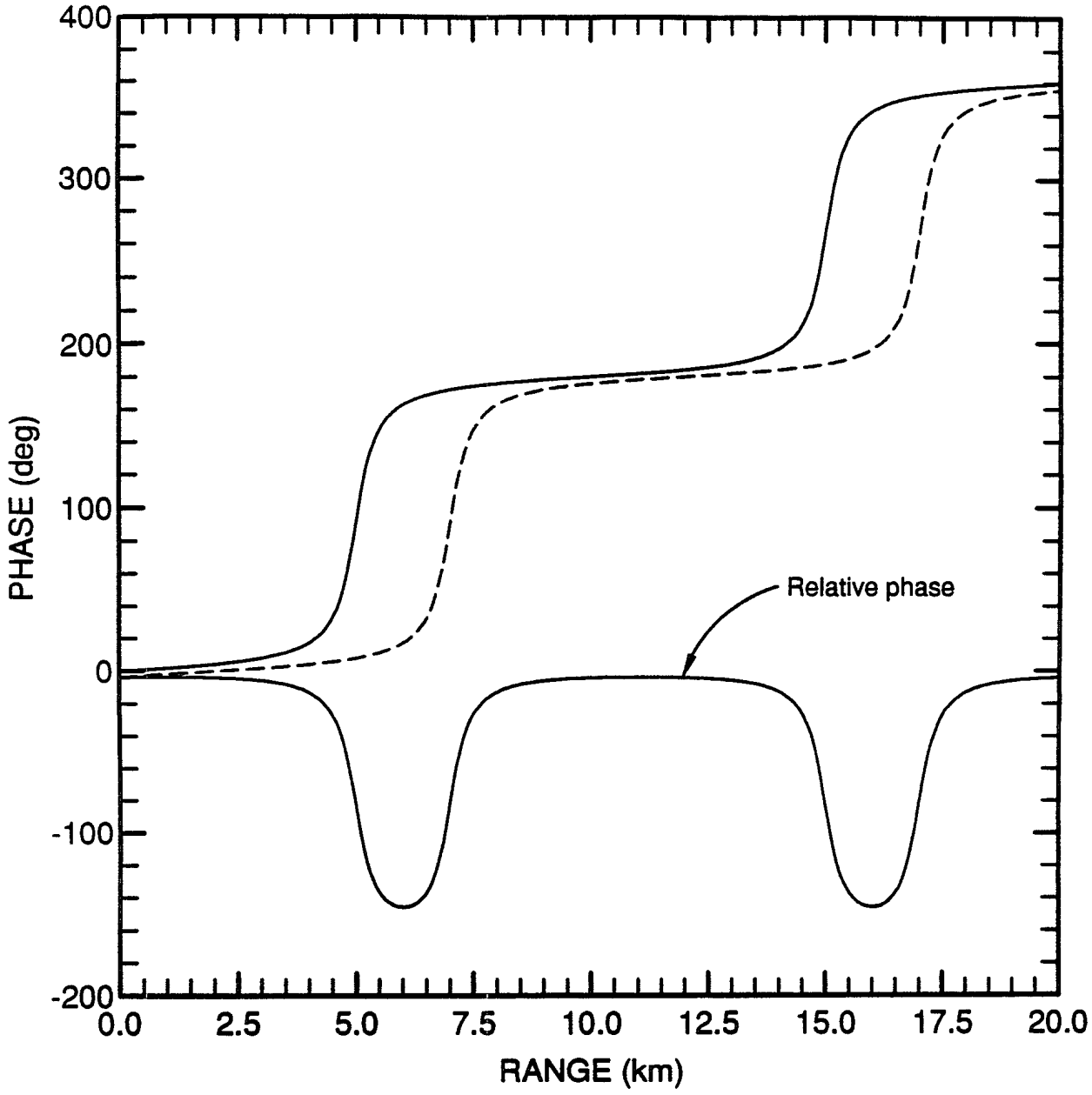

Fig. 5. Illustration of the phase swing in the relative phase. Upper solid and dashed lines are the absolute phases at hydrophones x and y respectively, with $\alpha = 0.1$. Lower solid line is the relative phase obtained by subtracting the upper solid line from the dashed line.

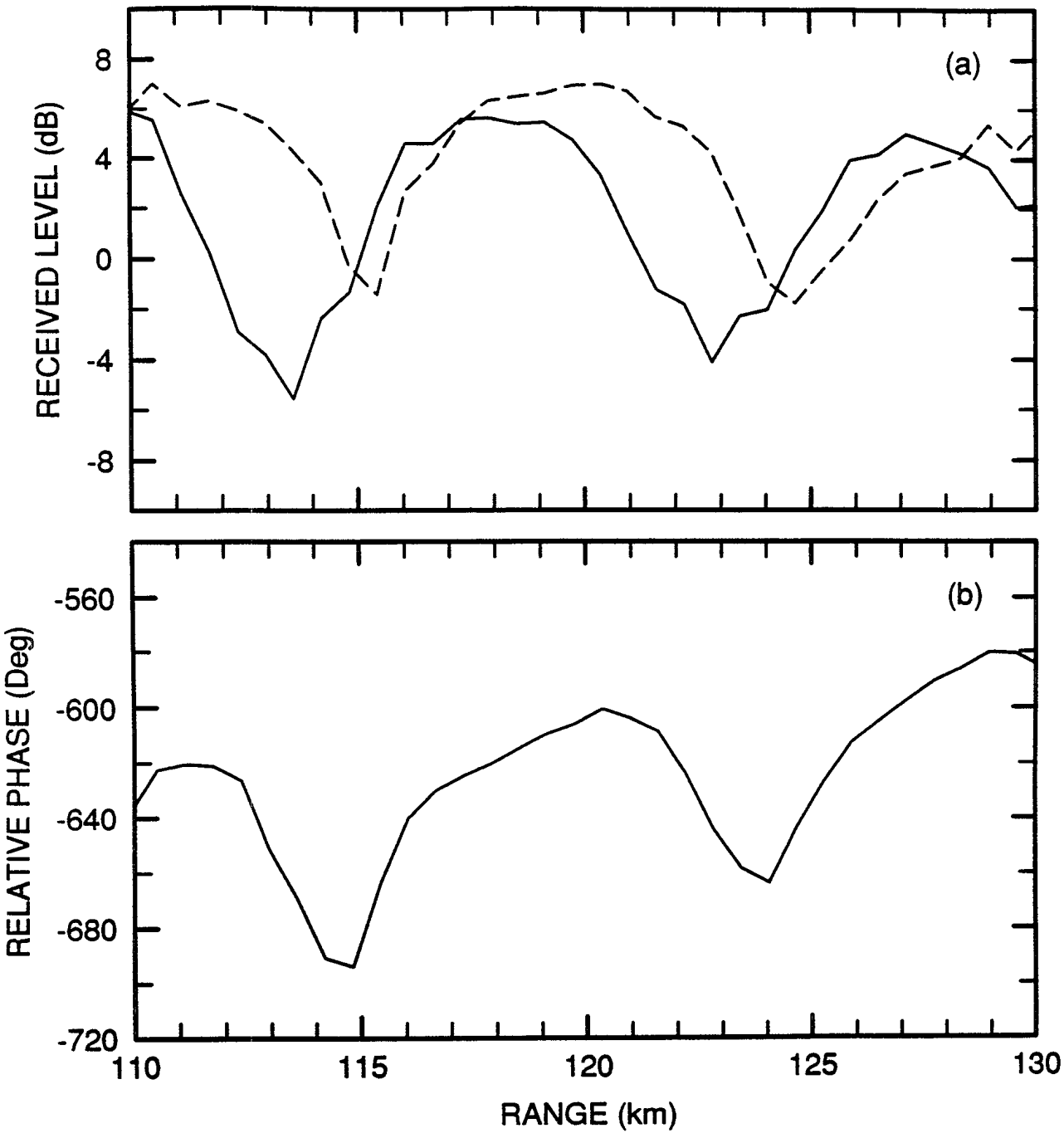

Fig. 6. Large scale reproduction of Fig. 2.

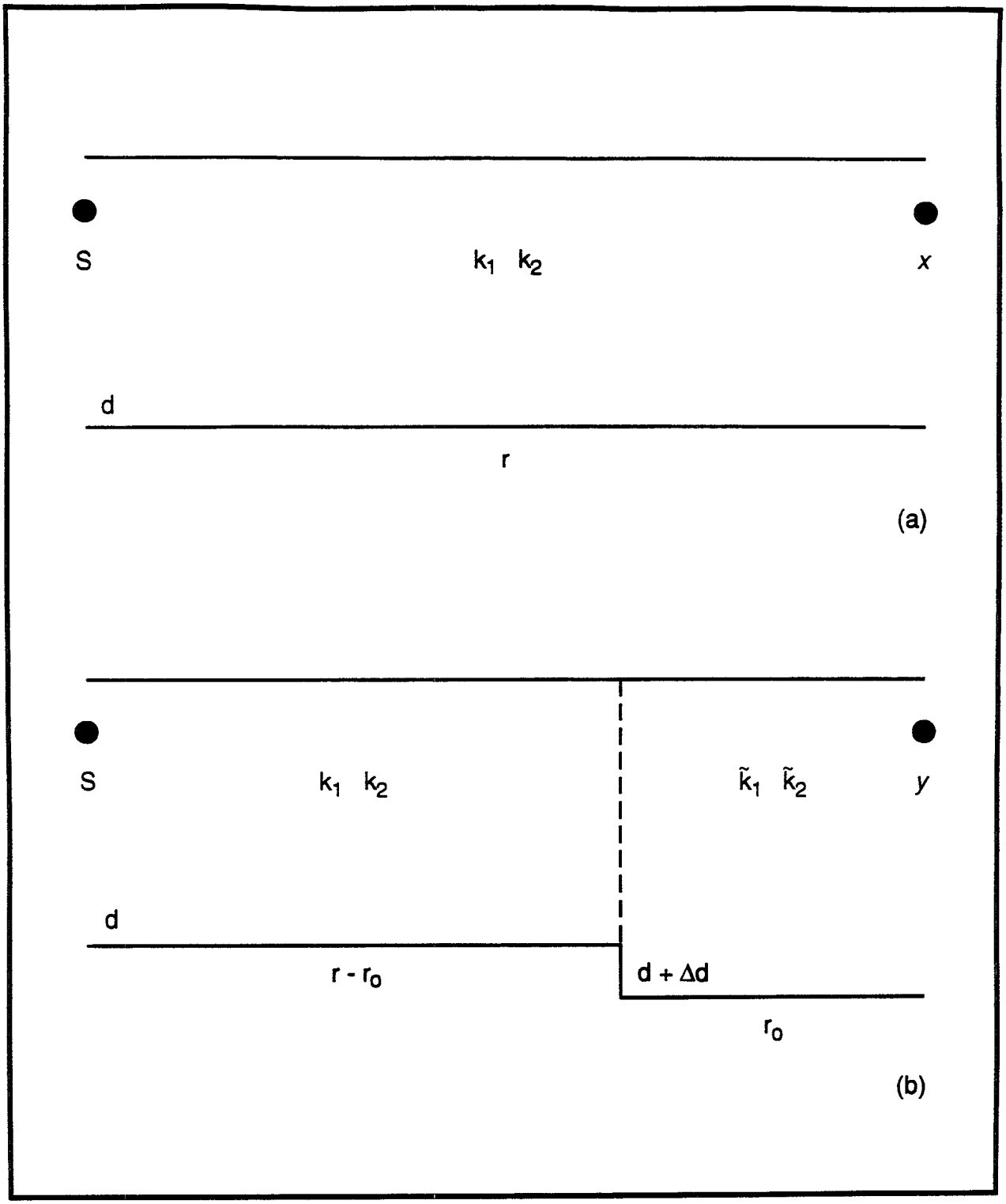

Fig. 7. Diagram of the waveguide, showing the propagation path to (a) hydrophone x and (b) hydrophone y.

expression in Eq. (3),

$$p_x(r) = \frac{1}{\sqrt{r}}(a_1 e^{ik_1 r} + a_2 e^{ik_2 r}). \tag{12}$$

On the other hand, the bottom over which the signal travels to hydrophone y is initially of depth d but then deepens to $d + \Delta d$ over a range interval r_o, where the depth change Δd is assumed to be small. In the real bathymetry, the bottom would make a gradual transition from depth d to $d+\Delta d$, but for simplicity this has been modelled by the sudden change in Fig. 7. As shown in the figure, the wavenumbers k_1 and k_2 will be associated with the water depth d, and the wavenumbers $\tilde{k}_1$ and $\tilde{k}_2$ with the water depth $d + \Delta d$. We shall put $\tilde{k}_j = k_j + \epsilon_j$, where ϵ_j is the perturbation in the wavenumber caused by the depth change. Also, because the depth change Δd is small, the adiabatic approximation[2] will be used to derive an expression for the pressure at hydrophone y. It can be shown that this leads to the expression

$$p_y(r) = \frac{1}{\sqrt{r}}(b_1 e^{ik_1 r} + b_2 e^{ik_2 r}), \tag{13}$$

where

$$b_j = a_j \exp(i\epsilon_j r_o), \qquad \text{for } j = 1,\ 2. \tag{14}$$

Equation (13) is valid only for $r \geq r_o$. In deriving Eq. (13), it was further assumed that the mode functions are negligibly affected in the upper portion of the water column by the depth change.

The phases θ_x and θ_y of Eq. (11) will still have the form shown in Eq. (7), but now the propagation constants differ for the two cases. The constants will be distinguished by subscripts x and y, although when the constants are the same for both cases, the subscript will be omitted. We consider the constants one by one:

i) A comparison of Eqs. (12) and (13) shows that $\overline{k}_x = \overline{k}_y = \overline{k}$, and similarly for Δk. Hence, the distance between nulls as measured by the two hydrophones will be the same, as it depends on the depth of the water in which the source moves, not on the depth of the water in which the receivers are located.

ii) Equation (14) shows that the coefficients b_j differ from the a_j by only a phase shift, so that $|a_j| = |b_j|$. It then follows from Eq. (8) that $\alpha_x = \alpha_y = \alpha$.

iii) Because we are interested in relative effects, we may take the modal coefficients a_j to be real-valued. (The absolute range of the nulls from the source may then be incorrect, but for relative effects between hydrophones x and y this does not matter.) Then $\overline{\psi}_x = 0$ and $\Delta\psi_x = 0$. From Eq. (14) it is easily shown that $\overline{\psi}_y = \overline{\epsilon}\, r_o$ and $\Delta\psi_y = r_o \Delta\epsilon$, where $\overline{\epsilon}$ and $\Delta\epsilon$ are defined from Eq. (4) in an obvious way.

In summary, the phases at hydrophones x and y are given by

$$\theta_x(r) = \overline{k}\, r + \tan^{-1}\left(\alpha \tan(r\Delta k)\right), \tag{15a}$$

$$\theta_y(r) = \overline{k}\, r + \overline{\epsilon}\, r_o + \tan^{-1}\left(\alpha \tan(r\Delta k + r_o\Delta\epsilon)\right). \tag{15b}$$

The relative phase of Eq. (11) will therefore have a constant phase offset $\overline{k}\Delta r + \overline{\epsilon}\, r_o$ and a fluctuating component arising from the subtraction of the last terms in Eqs. (15a) and (15b). The only difference from the case illustrated in Fig. 4 is that the term $r_o\Delta\epsilon$ is present in the argument of Eq. (15b). This term causes a shift of the pressure field in addition to that caused by the hydrophone offset Δr. This additional range shift is equivalent to a range offset Δr_{eq} defined by

$$r_o\Delta\epsilon = \Delta r_{eq}\Delta k.$$

This yields the result

$$\Delta r_{eq} = r_o\, \frac{\Delta\epsilon}{\Delta k} \tag{16}$$

for the apparent range shift caused by the depth change in Fig. 7. The total range shift is then given by $\Delta r + \Delta r_{eq}$.

3.4 Comparison of the model with the data

This completes the derivation of the propagation model, and it remains only to compare the predicted results with the real data. Based on the knowledge of the experimental site, the values $d = 500$ m and $\Delta d = 100$ m were chosen. That is, hydrophones x and y are in 500 m and 600 m of water respectively. The program SNAP was used to compute the wavenumbers for the two modes for the measured sound-speed profile. The wavenumber values are given in Table I. In this table, the k_j are the wavenumbers for the 500 m depth and the ϵ_j are the perturbations for the 600 m depth. The last line in the table gives the differences $k_1 - k_2$ and $\epsilon_1 - \epsilon_2$; the values Δk and $\Delta\epsilon$ follow upon division by 2. Recall that the total range shift between the interference patterns of the real data was -1.8 km. Based on a hydrophone offset $\Delta r \cong -0.1$ km as described earlier, this requires an equivalent range offset of -1.7 km due to the depth change. It is found that the ratio $\Delta\epsilon/\Delta k \cong -0.1398$, and hence from Eq. (16) that a value $r_o = 12$ km yields an equivalent range offset of the desired -1.7 km. As mentioned in the last section, it should be noted that the range shift in the experimental data would be due to a gradual depth transition over a range interval larger than 12 km.

Figure 8 shows the results produced by the analytic model, both for the pressure magnitudes and for the relative phase. This figure should be compared with the experimental

Table I. Propagation parameters.

	k_j (m^{-1})	ϵ_j (m^{-1})
$j = 1$	0.1040942018	0.0000013126
$j = 2$	0.1033364705	0.0001072282
Difference	0.0007577313	−0.0001059156

data in Fig. 6. In producing Fig. 8, the value of α, which determines the abruptness and extent of the phase swing, was adjusted until the modelled results agreed well with the experimental data. The final value of α was set to $\frac{1}{3}$, as used in Fig. 4. It is clear that the broad features of the experimental data are reproduced quite well by the simple two-mode model with an abrupt depth change in the waveguide.

Note from the two figures that the model does not accurately predict the distance between the nulls in the pressure field. As discussed earlier, the source was in fact located in deeper water over the continental slope, whereas we have modelled only that part of the propagation that takes place on the continental shelf. Since the distance between the nulls in the pressure field is determined by the depth of the water in which the source moves, our simple model does not adequately predict this distance. For this same reason, the value of α could not be computed from the mode functions given by SNAP for a range-independent environment. However, incorporating the continental slope into the model would preclude the simple analytical treatment that has provided insight into the phase-swing phenomenon.

4. SUMMARY

A propagation-loss experiment was conducted in which a narrowband source moved away from an array of hydrophones located in shallow water. It was found that the relative phase between the signals received at two widely separated hydrophones underwent rapid swings near the nulls of the pressure field. It was shown that a simple two-mode propagation model could explain the source of these phase swings, but that the range offset of the two hydrophones was insufficient to account for the observed magnitude of the swings. However, it was demonstrated that the experimental data could be fit quite well with the two-mode model by introducing different bathymetries along the propagation paths to the two hydrophones. The effect of differing bathymetries is to produce a relative shift between the pressure fields observed at the two hydrophones, similar to what would be observed if the range offset between hydrophones were increased.

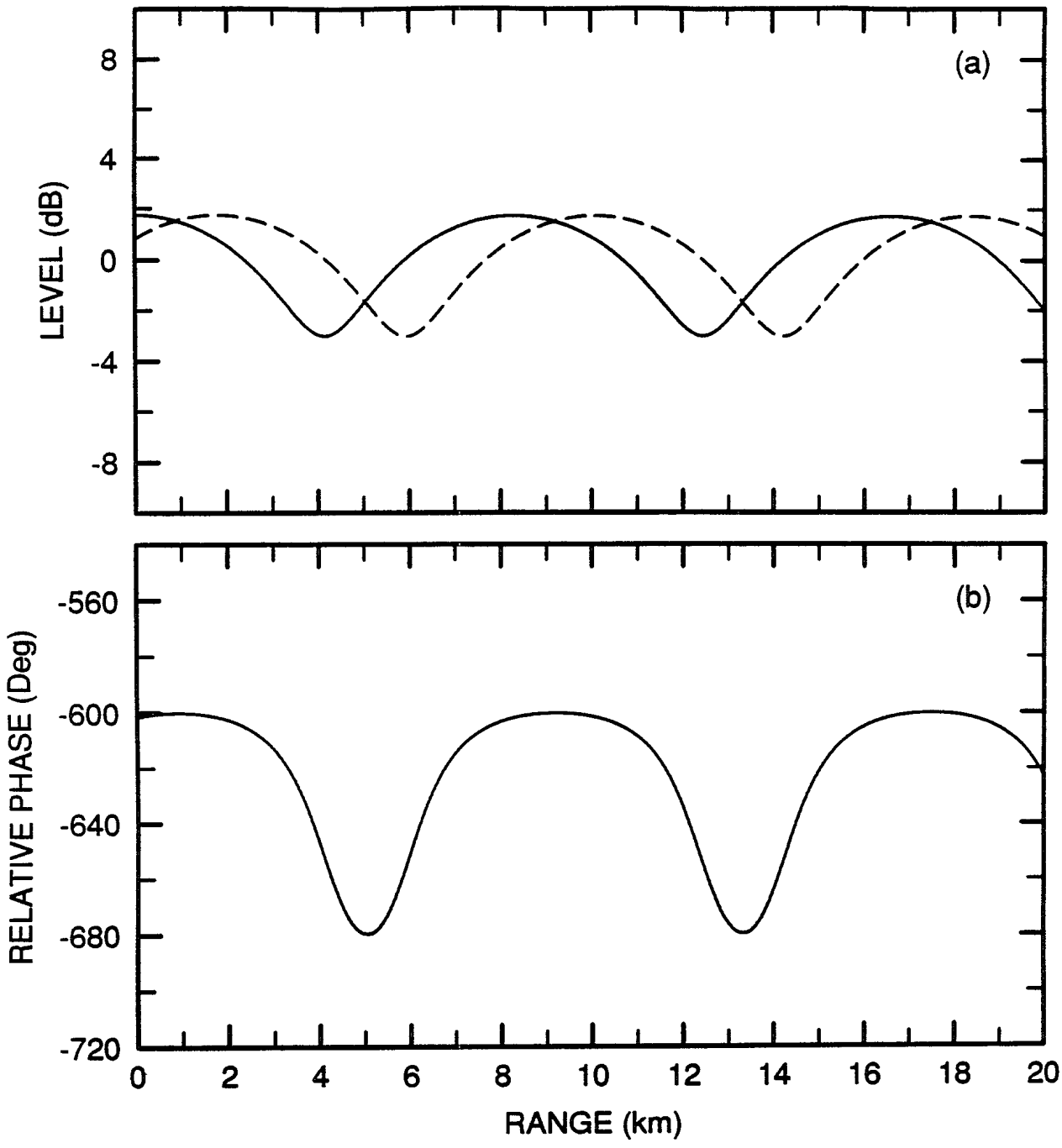

Fig. 8. (a) Modelled level vs source range for hydrophones x and y (solid and dashed curves respectively). (b) Modelled phase at hydrophone y relative to that at hydrophone x.

REFERENCES

1. G.V. Frisk, J.F. Lynch, and J.A. Doutt, "The determination of geoacoustic models in shallow water," in *Ocean Seismo-Acoustics*, edited by T. Akal and J.M. Berkson (Plenum, New York, 1986), pp. 693–702.

2. F.B. Jensen and M.C. Ferla, "SNAP: The SACLANTCEN normal-mode acoustic propagation model," SACLANTCEN ASW Research Centre, San Bartolomeo, Italy, Memorandum SM–121, 1979.

DISTRIBUTION

REPORT NUMBER:	Technical Memorandum 94–117
TITLE:	A Simple Model for the Prediction of Phase Swings Observed in Acoustic Propagation Data
AUTHORS:	Brian H. Maranda and Gordon R. Ebbeson
DATED:	July 1994

1 – DSIS
1 – DRDM
1 – DMCS–3
1 – DMOR
2 – DREA
10 – DREP

Unclassified

SECURITY CLASSIFICATION OF FORM
(highest classification of Title, Abstract, Keywords)

DOCUMENT CONTROL DATA

(Security classification of title, body of abstract and indexing annotation must be entered when the overall document is classified)

1. ORIGINATOR (the name and address of the organization preparing the document. Organizations for whom the document was prepared, e.g. Establishment sponsoring a contractor's report, or tasking agency, are entered in section 8.)

Defence Research Establishment Pacific
FMO Victoria, B.C.
V0S 1B0

2. SECURITY CLASSIFICATION (overall security classification of the document including special warning terms if applicable)

Unclassified

3. TITLE (the complete document title as indicated on the title page. Its classification should be indicated by the appropriate abbreviation (S,C,R or U) in parentheses after the title.)

A simple model for the prediction of phase swings observed in acoustic propagation data (U)

4. AUTHORS (Last name, first name, middle initial)

Maranda, Brian H. and Ebbeson, Gordon R.

5. DATE OF PUBLICATION (month and year of publication of document)	6a. NO. OF PAGES (total containing information. Include Annexes, Appendices, etc.)	6b. NO. OF REFS (total cited in document)
July 1994	18	2

7. DESCRIPTIVE NOTES (the category of the document, e.g. technical report, technical note or memorandum. If appropriate, enter the type of report, e.g. interim, progress, summary, annual or final. Give the inclusive dates when a specific reporting period is covered.)

Technical Memorandum

8. SPONSORING ACTIVITY (the name of the department project office or laboratory sponsoring the research and development. Include the address.)

9a. PROJECT OR GRANT NO. (if appropriate, the applicable research and development project or grant number under which the document was written. Please specify whether project or grant)	9b. CONTRACT NO. (if appropriate, the applicable number under which the document was written)
DRDM-08	

10a. ORIGINATOR'S DOCUMENT NUMBER (the official document number by which the document is identified by the originating activity. This number must be unique to this document.)	10b. OTHER DOCUMENT NOS. (Any other numbers which may be assigned this document either by the originator or by the sponsor)
DREP TM 94-117	

11. DOCUMENT AVAILABILITY (any limitations on further dissemination of the document, other than those imposed by security classification)

(X) Unlimited distribution
( ) Distribution limited to defence departments and defence contractors; further distribution only as approved
( ) Distribution limited to defence departments and Canadian defence contractors; further distribution only as approved
( ) Distribution limited to government departments and agencies; further distribution only as approved
( ) Distribution limited to defence departments; further distribution only as approved
( ) Other (please specify):

12. DOCUMENT ANNOUNCEMENT (any limitation to the bibliographic announcement of this document. This will normally correspond to the Document Availability (11). However, where further distribution (beyond the audience specified in 11) is possible, a wider announcement audience may be selected.)

Unlimited

Unclassified

SECURITY CLASSIFICATION OF FORM

DCD03 2/06/87

13. ABSTRACT (a brief and factual summary of the document. It may also appear elsewhere in the body of the document itself. It is highly desirable that the abstract of classified documents be unclassified. Each paragraph of the abstract shall begin with an indication of the security classification of the information in the paragraph (unless the document itself is unclassified) represented as (S), (C), (R), or (U). It is not necessary to include here abstracts in both offical languages unless the text is bilingual).

In 1986, a propagation loss experiment was conducted in which a narrowband source moved away from two widely separated hydrophones located in shallow water. It was found that the relative phase between the signals received at the two hydrophones underwent rapid swings near the nulls of the pressure field. In this paper, a simple two-mode propagation model is derived that explains the source of these phase swings. In order to produce phase swings as large as those observed in the experimental data, it was necessary to introduce different bathymetries along the propagation paths to the two hydrophones.

(See report for French version of the abstract.)

14. KEYWORDS, DESCRIPTORS or IDENTIFIERS (technically meaningful terms or short phrases that characterize a document and could be helpful in cataloguing the document. They should be selected so that no security classification is required. Identifiers, such as equipment model designation, trade name, military project code name, geographic location may also be included. If possible keywords should be selected from a published thesaurus. e.g. Thesaurus of Engineering and Scientific Terms (TEST) and that thesaurus-identified. If it is not possible to select indexing terms which are Unclassified, the classification of each should be indicated as with the title.)

Acoustics
Modal interference
Modes
Phase
Propagation
Underwater